KKU Res.j. 2015; 20(3) : 346-359
http://resjournal.kku.ac.th

Giant Dielectric, Low Loss Tangent and Non-Ohmics Properties of $CaCu_3Ti_{4.7}O_{12}$ Ceramics Prepared by Polymer Pyrolysis Method

*Sunan Nonglek[1],Sasitorn Putjuso[2] and Thanin Putjuso[2]**

[1]Faculty of industrial and Technology, Rajamangala University of Technology Rattanakosin, Wang Klai Kangwon Campus, 77110, Thailand
[2]School of General Science, Faculty of Liberal Arts, Rajamangala University of Technology Rattanakosin, Wang Klai Kangwon Campus, 77110, Thailand
**Correspondent author: putjuso@hotmail.com; Thanin.put@rmutr.ac.th*

Abstract

In this work, $CaCu_3Ti_{4.7}O_{12}$ (CCT4.7O) powder was prepared by polymer pyrolysis method. The influence of phase composition and microstructure were characterized using X-ray diffraction (XRD) and scanning electron microscopy (SEM). The results show that the TiO_2 secondary phase has a remarkable on the microstructure, dielectric loss tangent (tanδ) and dielectric constant (ε′) of CCT4.7O ceramics, respectively. Interestingly, low dielectric loss tangent of ~ 0.03 and giant dielectric constant of 31,908 with temperature coefficients less than ± 15% in the temperature range of −50 – 90 ˚C are observed in a ceramic sintered at 1060 ˚C for 10 h (CCT4.7O-2). Both of ceramics sintered at 1060 ˚C for 6 h (CCT4.7O-1) and 10 h (CCT4.7O-2) display a non linear current voltage with the non-linear coefficient (α) and breakdown field (E_b) values of 6.4, 5.6 and 1554, 1020, respectively. The dielectric constant, electrical response of grain boundaries, and related nonlinear current–voltage behavior are found to be associated with the microstructure of CCT4.7O ceramics.

Keywords: *Dielectric, dielectric loss tangent, non-ohmics, polymer pyrolysis*

1. Introduction

Recently, giant dielectric materials have a significant role in microelectronic devices such as ultra capacitors in hybrid-electric vehicles, pulsed power systems and memory (DRAM) devices. Among giant dielectric materials studied in recent years, $CaCu_3Ti_4O_{12}$ (CCTO) has attracted much attention because of its high dielectric constant (10^4–10^5) at room temperature and good stability over a wide range of temperature (-173 ˚C to 327 ˚C)[1,2]. In addition, below -173 ˚C, the dielectric constant drops rapidly to around 100 without any structural phase transition[3]. To date, several explanations for the origin of the giant dielectric response in the CCTO ceramics is due to the Maxwell–Wagner polarization effect. This polarization can be introduced at several sites[4], mainly through the internal interfaces inside the ceramics such as grain boundaries (GBs), domain boundaries (DBs), and at the external interfaces such as sample–electrode interfaces. Moreover, the internal barrier layer capacitor (IBLC) model representing semiconducting grains and insulating grain boundaries[2] confirms the electrical heterogeneities in the microstructure of CCTO, and it has been widely accepted as the most likely explanation for the abnormal dielectric response in CCTO. In addition to the giant dielectric properties, CCTO material can also exhibit non–linear electrical behavior due to the inhomogeneous features at the grain boundaries i.e. the Schottky effect, making them suitable for varistor applications[1,5]. In general, CCTO materials occupy not only a high dielectric constant but also a large dielectric loss tangent (tanδ) which is obstacle for the practical application[6,7]. Thus, reducing of tan δ value in this material is one of a key point to make it suitable for commercial application. According to this, some researchers are successful in reducing the dielectric loss of CCTO by the use of various dopants such as Sr[8], Sm[9] and Zr[10]. Besides the doping effect on the cation site, Ca deficiency and Ca excess[11], Cu excess[12], Cu deficiency[13] Ti deficiency[14], and the Ti excess[15], effects have been also studied on the dielectric response of CCTO. The Ca-deficiency and -excess in CCTO can result in a higher and lower dielectric constant, while the tanδ value is suppressed by a Ca-deficiency[11]. The Cu ions in CCTO appear to play a very important role as the segregation of copper oxide at the grain boundaries and it is believed to be responsible for the high resistance associated with the grain boundary[12,13]. The Ti-deficiency in CCTO can result in a lower dielectric constant[14], while the Ti-rich CCTO ceramic[15] exhibits higher dielectric response. However, the effect of stoichiometry i.e. the relative amount of Ca, Cu and Ti is not fully studied. Among the deficiency and excess of caions (Ca, Cu and Ti) in CCTO ceramic, the Ti-excess is very interesting, because it can improve the dielectric and suppressed the tanδ value. **As previously reported,** the Ti-deficiency and excess in CCTO ceramics have been generally prepared by the standard solid-state reaction method[14,15]. In this method, high sintering temperatures and long reaction times are required to produce complete reactions to form a pure CCTO phase. Up to now, many chemical techniques play an important role in the preparation of CCTO giant dielectric material[16,17]. Polymer pyrolysis is one chemical process, which has the advantages over others technique, because of the ease of operation, batch scalability, and it can be

used to produce highly homogeneous nanocrystalline material. Recently, this polymer pyrolysis method was used to synthesize nanocrystalline of composite CCTO/CTO ceramics[18] and CCTO ceramic[19] with low tanδ. To our knowledge, there has been no prior work on the study of the dielectric, tanδ and non-linear properties of Ti-excess in CCTO ceramics preparing by the polymer pyrolysis route.

In this paper, we report the synthesis of $CaCu_3Ti_{4.7}O_{12}$ (CCT4.7O) powder prepared by polymer pyrolysis method. The CCT4.7O ceramics are obtained by sintering the 850 ˚C-precalcined CC4.7TO powder at the appropriate temperature of 1060 ˚C for 6 and 10 h in air. The effect of sintering time on the microstructure, dielectric response, electrical properties, and non–linear characteristic of the CCT4.7O ceramics are systematically investigated. The results reveal that the CCT4.7O ceramics exhibit giant dielectric with low loss tangent (tanδ) and the effect of sintering condition on the dielectric and non–linear properties are closely related to the CCT4.7O microstructural evolution.

2. Materials and methods

In this work, $CaCu_3Ti_{4.7}O_{12}$ (CCT4.7O) powder was prepared by the polymer pyrolysis method. Copper nitrate ($Cu(NO_3)_2.3H_2O$ 99.5% Carlo Erba), calcium nitrate ($Ca(NO_3)_2.4H_2O$, 99.99% Kanto), titanium solution ($C_{16}H_{28}O_6Ti$ 75 wt.% in isopropanol), ammonium persulfate ($(NH_4)_2S_2O_4$, 99.99% Sigma Aldrich) and acrylic acid were used as the starting materials. Firstly, a stoichiometric amount of $C_{16}H_{28}O_6Ti$ (27 mL) was mixed in an acrylic aqueous acid solution (30 mL) under constant stirring at room temperature. Secondly, stoichiometric amounts of $Ca(NO_3)_2 \cdot 4H_2O$ (3.142 g) and $Cu(NO_3)_2.3H_2O$ (5.46 g) were dissolved in the pre-mixed solution under constant stirring at 100 ˚C until a clear solution was obtained. Then, several drops of an aqueous 5% $(NH_4)_2S_2O_4$ solution (12 mL) were added to the mixed acrylic acid solution as an initiator to promote polymerization[19]. The obtained gel precursor was dried at 350 ˚C in a box furnace for 2 h. The dried gel was ground and then calcined at 850 ˚C for 9 h in air using heating and cooling rate 5˚C/min. The CCT4.7O powder was pressed into pellets of 9.5 mm in diameter and 1 mm in thickness using uniaxial compression at 150 MPa. Finally, the CCT4.7O ceramics sintered in air at 1060 ˚C (using heating and cooling rate of 5 ˚C/min) for 6 h and 10 h were abbreviated as CCT4.7O-1and CCT4.7O-2, respectively. The density of both ceramics was measured by Archimedes method.

Phase composition of CCT4.7O powder and ceramic samples were characterized by X-ray diffraction (PW3040 Philips X-ray diffractometer with CuKα radiation (λ = 0.15406 nm), the Netherlands). Surface morphologies as well as chemical elements in the CCT4.7O ceramics at different areas were studied and analyzed by scanning electron microscopy (LEO SEM VP1450, UK) and energy dispersive X-ray spectroscopy (EDS), respectively. The dielectric and electrical properties of the samples were measured using a Hewlett Packard 4194A impedance gain phase analyzer over a wide range of frequency (100 Hz-1MHz) and temperature (-50 to 200 ˚C) at an oscillation voltage of 0.5 V. During the measurement, temperature was kept constant with an accuracy of ± 0.5 ˚C.

Prior to the dielectric measurements, both surfaces of ceramic pellets were subsequently polished, washed, dried and coated with Au using a Polaron SC500 sputter coating unit. Current–voltage measurements were performed at room temperature using a high voltage measurement unit (Keithley Model 247). Breakdown electric field (E_b) was obtained at a current density (J) of 1 mA.cm^{-2}. The nonlinear coefficient (α) values were calculated by the following equation,

$$\alpha = \frac{\log(J_2 / J_1)}{\log(E_2 / E_1)} \quad (1)$$

where E_1 and E_2 are the electric fields corresponding to $J_1 = 1$ and $J_2 = 10$ mA.cm^{-2}, respectively.

The complex permittivity (ε') was calculated by the following equation,

$$\varepsilon^* = \varepsilon' - i\varepsilon'' = \frac{1}{i\omega C_0 Z^*} = \frac{1}{i\omega C_0 (Z' - iZ'')} \quad (2)$$

The dielectric constant (ε') and the dielectric loss (ε') were calculated by

$$\varepsilon' = \frac{C_p d}{\varepsilon_0 A} \quad (3)$$

$$\varepsilon'' = \varepsilon' \times tan\,\delta \quad (4)$$

where C_p is the measured capacitance of each pellet, ε_0 is the permittivity of free space, A is the surface area of the electrode and d is the thickness of each pellet.

3. Results and discussion

3.1 XRD Characterization

The XRD patterns of the CCT4.7O powder (P-850), sintered CCT4.7O ceramic samples (CCT4.7O-1 and CCT4.7O-2) and the standard CCTO (ICSD card No.95714) are shown in Fig. 1. The second phases of TiO_2 (ICSD card No.62679) and CuO (ICSD card No.26715) are observed in P-850 powder, as shown in Fig. 1(b). The presence of TiO_2 comes from an excess of Ti content in the solution[20], resulting in the formation of the CuO phase due to the deviation of the components from the stoichiometric formula. The CuO secondary phase can be suppressed by sintering time. As clearly shown in Fig. 1 (c) and (d), the intensity of a diffraction peak of CuO observed at 2θ ~ 35.5 in the CCT4.7O-2 ceramic is lower than that found in the CCT4.7O-1 ceramic. However, the TiO_2 diffraction peaks are still observed in both CCT4.7O ceramics. It is suggested that, the TiO_2 secondary phase is stable and separated from the main CCTO phase, and it cannot be affected by the sintering temperature and time. From the X-ray line broadening of the main peaks (220), (400) and (422), the average crystallite size of the P-850 powder is calculated using Scherrer's formula[19] and it is found to be 86.3 ± 6 nm. The lattice parameters a of the P-850, CCT4.7O-1and CCT4.7O-2 samples are estimated using the Rietveld program and they are found to be 7.391, 7.387 and 7.386 Å, respectively. These values are comparable to those reported in the literature[19] and ICSD card no. 95714 for standard CCTO (7.391 Å). Using the Rietveld method, the calculated density of CCT4.7O ceramic is 5.056 g.cm^{-3}. The relative densities of CCT4.7O-1and CCT4.7O-2 ceramics measured by the Archimedes method are found to be 87.4% and 89.5%, respectively. The relative density, X-ray density and lattice parameter of these samples are summarized in Table I.

Table I. Dielectric constant (ε') and dielectric loss tangent (tanδ) at 30 ˚C and 1 kHz), Grain (R_g) and Grain boundary (R_{gb}) resistances at 150 ˚C, non–linear coefficient (α), and breakdown field (E_b) for the CCT4.7O ceramics prepared by polymer pyrolysis method

Sample	ε'	tanδ	Resistance at 150 ˚C (Ω.cm)		α	E_b (V.cm^{-1})
			R_g	R_{gb}		
CCT4.7O-1	21,000	0.07	85	86,900	6.4	1554
CCT4.7O-2	31,908	0.03	18	31,300	5.6	1020

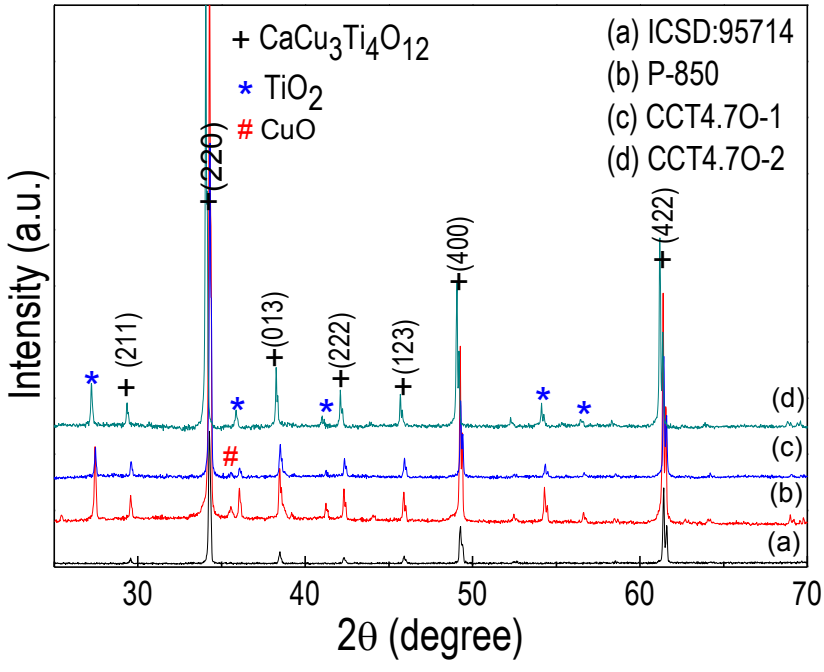

Figure 1. XRD patterns of (a) standard CCTO (ICSD: 95714) (b) P-850, (c) CCT4.7O-1 and (d) CCT4.7O-2 samples.

3.2 SEM-EDS Characterization

Fig. 2(a) and (b) show the surface morphologies of the CCT4.7O-1 and CCT4.7O-2 ceramics, respectively. As can be seen in Fig. 2(a) and (b), both CCT4.7O-1 and CCT4.7O-2 ceramics show the microstructure consisting of coarse grains with sizes in the range of 4 - 17 μm surrounded by fine grains of 0.5 - 2 μm in size. The approximate percentage of fine grain is increased with increasing sintering time, as shown in Fig. 3 for the EDS analysis coarse grains (1) and fine grains (2) for the CCT4.7O-2 ceramic. In this figure, it is evident that the coarse grain region (region 1) is nearly stoichiometric, while the fine grain (region 2) is Cu rich.

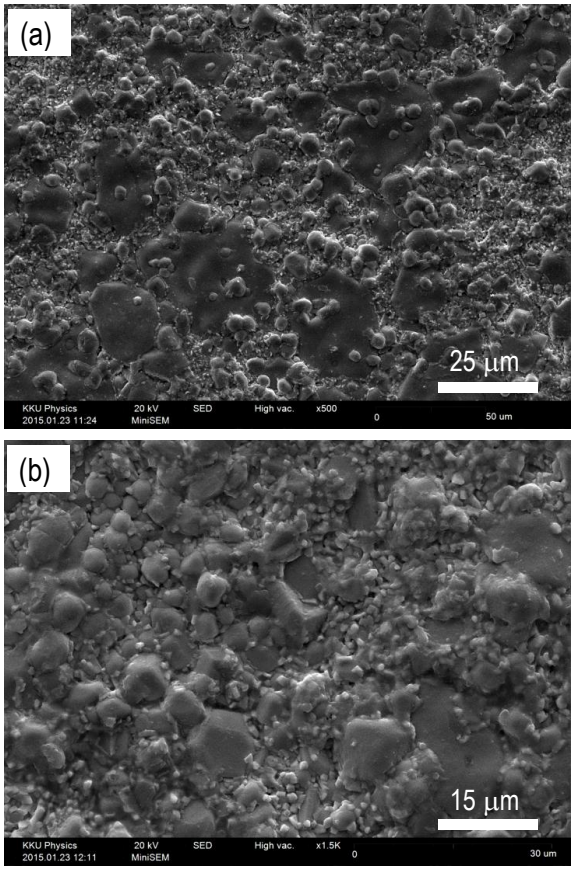

Figure 2. SEM images of (a) CCT4.7O-1 and (b) CCT4.7O-2 ceramics.

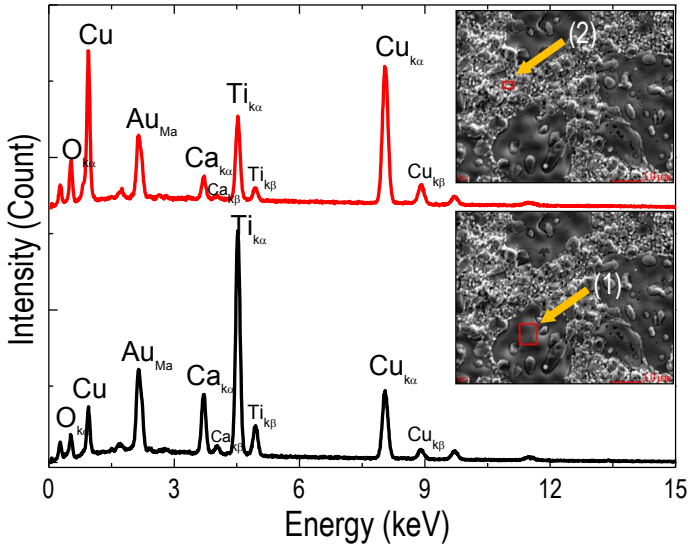

Figure 3. Representative EDS spectra of CCT4.7O-2 ceramics (1) coarse grain and (2) fine grain.

3.3 Dielectric properties

The frequency dependence of the dielectric constant (ε′) and loss tangent (tanδ) of CCT4.7O-1 and CCT4.7O-2 ceramics at 30 ˚C and 1 kHz are shown in Fig. 4. In Fig. 4, both values of ε′ and tanδ of the CCT4.7O-1 ceramic are 21,000 and 0.07, respectively. In the case of CCT4.7O-2 ceramic, these values are 31,908 and 0.03, respectively. In the present study, it is clear that the CCT4.7O-2 ceramic has a higher dielectric constant than that of the CCT4.7O-1 ceramic. This may be due to the denser microstructure of the CCT4.7O-2 ceramic, corresponding to the relatively high density of this ceramic. These tanδ values of CCT4.7O ceramics are in good agreement with those of the TiO_2-rich CCTO ceramic of 0.03[21], and lower than that of CCTO ceramic literature values of 0.043[19], 0.06[22]. These results indicate that CCT4.7O ceramics prepared by sintering the powder precursor of CCT4.7O obtained from polymer pyrolysis method might have a potential for capacitor application. The values of ε′ and tanδ at 30 ˚C and 1 kHz for both CCT4.7O-1 and CCT4.7O-2 ceramics are summarized in Table I. In general, it is widely accepted that the giant dielectric properties (high value of ε′ and low value of tanδ) of CCTO ceramics can be ascribed base on the internal barrier layer capacitor (IBLC) model[5,8,19]. The microstructures of both CCT4.7O ceramics are electrically heterogeneous, consisting of semiconductive part of grains and insulating layer of grain boundaries. Under an applied ac electric field, charges in the semiconducting grains are accumulated at the grain boundaries, resulting in the interfacial polarization at the interface between grain and grain boundary. This is responsible for the observed high dielectric response in both CCT4.7O ceramics. According to this electrical structure model, the effective dielectric constant can be expressed as $\varepsilon'_{eff} = \varepsilon_{gb} t_g / t_{gb}$,where ε_{gb}, t_g and t_{gb} are the dielectric constant of the grain boundary, the average grain size and the thickness of the grain boundary, respectively. Obviously, the increase in ε′ of the CCT4.7O-2 ceramic associates with the slight increase of the grain size, resulting from the increase of the sintering time. It is interesting that tanδ of CCT4.7O-2 ceramic is reduced by increasing sintering time, due to the higher content of TiO_2 second phase than that of the CCT4.7O-1 ceramic. This effect is in good agreement with the increase in the intensity peak of TiO_2 observed in the XRD results, as shown in Fig. 1. Fig. 5(a) shows the frequency dependence of ε' with temperature in the range of -50 to 100 ˚C for CCT4.7O-2 ceramic. It is observed that the variation of ε' ($\Delta\varepsilon'$) value at 1 kHz compared to the value at 30 ˚C for CCT4.7O-2 ceramic is found to be less than ± 15% in the temperature range of −50 to 90 ˚C (inset of Fig. 5(a)). However, the temperature variation of ε' is greater than ±15% when the temperature is increased to a value higher than 90 ˚C. As can be seen in Fig. 5(b) the relaxation peaks of ε'' in a low temperature range (-50 to 20 ˚C) for CCT4.7O-2 ceramic are shifted to a high frequency as a temperature is increased due to a thermally activated relaxation process. In this figure, the dielectric relaxation time (τ) can be calculated by the relations $\omega\tau = 1$ and $\omega = 2\pi f_p$, where f_p is a characteristic frequency corresponding to the peak of ε''. Generally, the temperature dependence of τ can be described by the Arrhenius law,

$$\tau = \tau_0 \exp(E_a / k_B T), \quad (5)$$

where E_a is the activation energy required for the relaxation process, τ_0 represents the pre-exponential factor, k_B is the Boltzmann constant, and T is the absolute temperature. From the relationship between Ln (τ) vs. 1000/T (inset of Fig. 5(b)) and using Eq. (5) the activation energy (E_a) can be calculated and they are found to be 0.065 and 0.101eV for CCT4.7O-1 and CCT4.7O-2 ceramics, respectively. These values are comparable to those reported in the literature for CCTO ceramics (E_a ~ 0.1 eV)[23] of the low temperature relaxation process.

The impedance complex plane plots (Z^* plots) at 30 ˚C and their expanded view at a high frequency for CCT4.7O-1 and CCT4.7O-2 ceramics are shown in Fig. 6(a) and inset of Fig. 6(a), respectively. In this figure, the grain resistance (R_g) can be estimated from a nonzero intercept on the Z′ axis at high frequencies (inset of Fig. 6(a)) (3) and they are found to be ~ 400 and ~ 50 Ω.cm for CCT4.7O-1 and CCT4.7O-2 ceramics, respectively. For the grain boundary (GB) resistance (R_{gb}), the complete semicircular arcs of CCT4.7O ceramics cannot be observed at 30 ˚C. However, the semicircular arcs of the R_{gb} value tend to decrease with increasing sintering temperature. As can be seen in Fig. 6(b), the completed semicircular arc of the R_{gb} for CCT4.7O-2 ceramic is reduced by increasing sintering temperature. It is important to note that R_g is estimated to be 5 to 6 orders of magnitude smaller than R_{gb}. As a result, it is reasonable to suggest that synthetic CCT4.7O ceramics are electrically heterogeneous, consisting of semiconducting grains and insulating GBs. Consequently, based on these experimental results, the giant ε' values of both CCT4.7O ceramics can be attributed to the effect of their special heterogeneous microstructure i.e. the different electrical characteristics between the grain and GB are suggested as a major contribution to observed giant ε'.

To investigate the electrical characteristics of grain boundaries, the frequency dependence of the imaginary part, Z″, of complex impedance Z^* is plotted. Z^* can be calculated by the following equation,

$$Z^* = Z' - jZ'' = \frac{1}{j\omega\varepsilon^* C_0}, \qquad (6)$$

where Z′ and Z″ are the real and imaginary parts of Z*, respectively. C_0 is defined by ε_0A/d. As shown in Fig. 6(c), Z″ peak is shifted to higher frequencies with increasing temperature, indicating a thermally activated electrical response. At the maximum value of Z″, it can be shown that $R = 2Z''_{max}$ [24]. Therefore, a decrease in Z''_{max} indicates a decrease in either grain resistance or grain boundary resistance. At a temperature of 150 ˚C, the calculated R_{gb} values are found to be 86.9 and 31.27 kΩ.cm for CCT3.7O-1 and CCT4.7O-2 ceramics, respectively. It is important to note that the R_{gb} value of CCT4.7O-1 ceramic is estimated to be 3 times higher than that of CCT3.7O-2 ceramic. This effect might be due to the presence of the CuO second phase in the CCT4.7O-1 ceramic, as shown by the XRD results in Fig. 1. CuO is generally well known to be segregated at the grain boundaries and it is suggested to be responsible for the high resistance associated at the grain boundary[12,13]. As shown in Fig. 6(d), the grain boundary conductivity, $\sigma_{gb} = 1/R_{gb}$, follows the Arrhenius law,

$$\sigma_{gb} = \sigma_0 \exp(\frac{-E_{gb}}{k_B T}), \qquad (7)$$

where σ_0 is the pre-exponential term, E_{gb} is the activation energy for conduction

at the grain boundaries, k_B is the Boltzmann constant, and T is the absolute temperature. The E_{gb} values of the CCT4.7O-1 and CCT4.7O-2 ceramics are calculated from the slope of the plots of σ_{gb} vs. 1000/T, and they are found to be 0.57 and 0.66 eV, respectively. These two values of E_{gb} are comparable to those reported values of 0.678[25] and 0.662 eV[26] for the grain boundaries of CCTO ceramics. As a result, it is obvious that CCT4.7O-2 ceramic posseses the highest E_{gb} value due to its relatively higher dielectric constant.

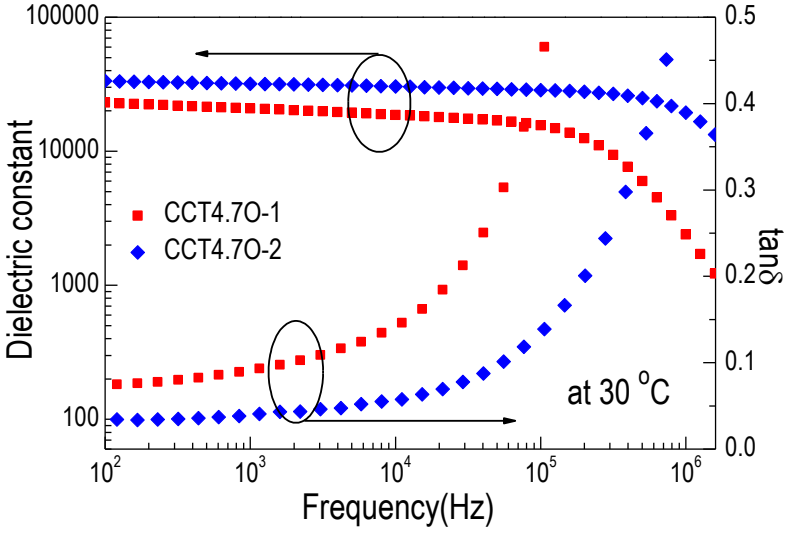

Figure 4. Frequency dependence of dielectric constant (ε') and dielectric loss tangent (tanδ) at 30 ˚C and 1 kHz of CCT4.7O-1 and CCT4.7O-2 ceramics.

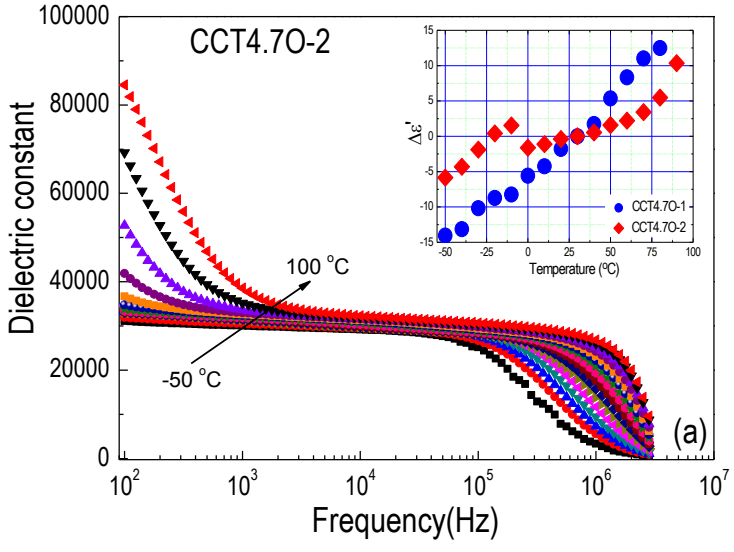

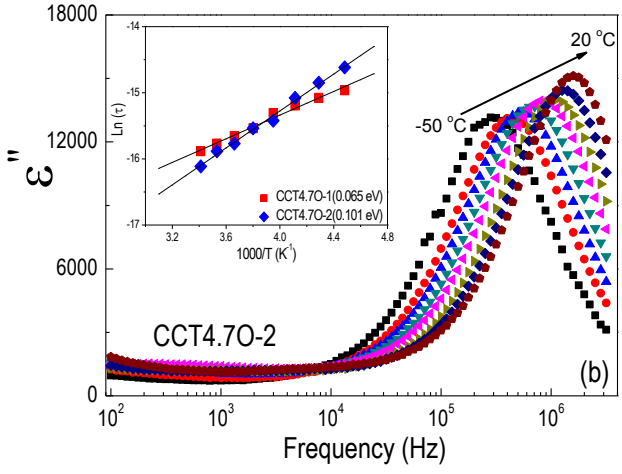

Figure 5. (a) Frequency dependence of the dielectric constant (ε') in the temperature range of −50 – 100 ˚C and (b) the dielectric loss (ε') in the temperature range of −50 – 20 ˚C of the CCT4.7O-2 ceramic; inset of (a) is the temperature coefficient ($\Delta\varepsilon'$) of both CCT4.7O ceramics in the temperature range of −50 – 90 ˚C evaluated at the frequency of 1 kHz, inset of (b) is the plot of Ln(τ) as a function of temperature for both of CCT4.7O ceramics.

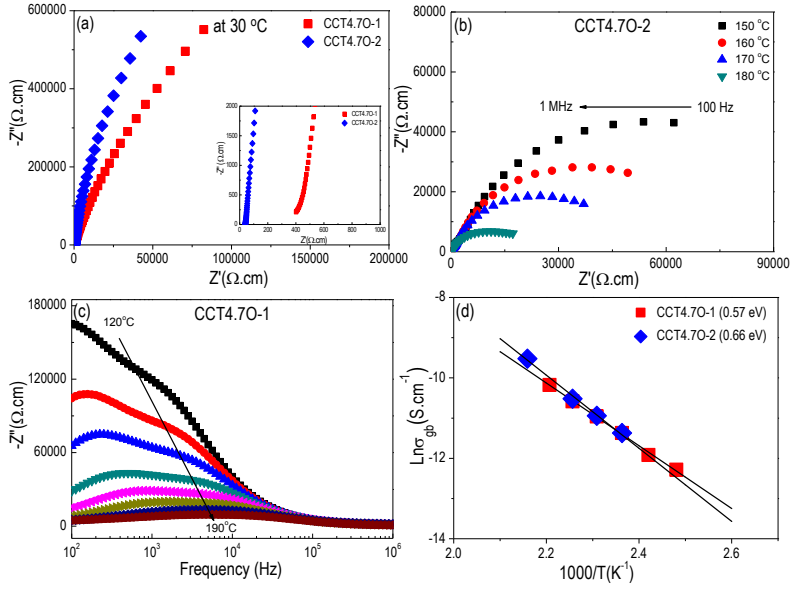

Figure 6. (a) and inset of (a) displays the impedance complex plane plot (Z^*) at 30 ˚C and the expanded view at a high frequency for both CCT4.7O ceramics; (b) is the impedance complex plane plot (Z^*) at various temperature in the range of 150-180 ˚C for CCT4.7O-2 ceramic; (c) displays the frequency dependence of Z" in the temperature range from 120 to 190 ˚C for CCT4.7O-1 ceramic (increasing step of measuring temperature is 10 ˚C); (d) shows the Arrhenius plot of Ln (s_{gb}) versus 1000/T for both of the CCT4.7O ceramics.

3.4 Non-linear properties

As shown in Fig. 7(a), both CCT4.7O ceramics exhibit non–Ohmic properties. The two most important parameters related to non–Ohmic properties, non–linear coefficient (α) and breakdown field (E_b) of the CCT4.7O ceramics can be calculated from these curves. As can be seen in Fig. 7(b), the relationship of current (current density, J) and voltage (electric field strength, E) for both of the CCT4.7O ceramics can be well characterized by the equation of varistor characteristic i.e. $I = KV^{\alpha}$, where K is a constant related to the electrical resistivity of the material. The α value is determined in the range of 1 – 10 $mA.cm^{-2}$ for CCT4.7O-1 and CCT4.7O-2 samples and they are found to be 6.4 and 5.6, respectively. These values are comparable to those reported in the literature of TiO_2 rich[15] and Ca rich[21] CCTO ceramics. The E_b values of CCT4.7O-1 and CCT4.7O-2 ceramics obtained at J = 1 $mA.cm^{-2}$ are 1,554 and 1,020 $V.cm^{-1}$, respectively. It is important to note that both α and E_b values are decreased with the increasing of grain sizes. This is in agreement with the results previously reported by Chung et al.[1] and Sun et al.[27]. In addition, both E_b and α values of CCT4.7O ceramics are decreased with the increase of sintering time, indicating the effect of sintering on the Schottky barrier[28]. It is worth noting that the value of E_b for the CCT4.7O-1 is higher than that of the CCT4.7O-2 ceramic. This result corresponds to the observation of a higher grain boundary resistance of the CCT4.7O-1 than that of the CCT4.7O-2 as sumarized in

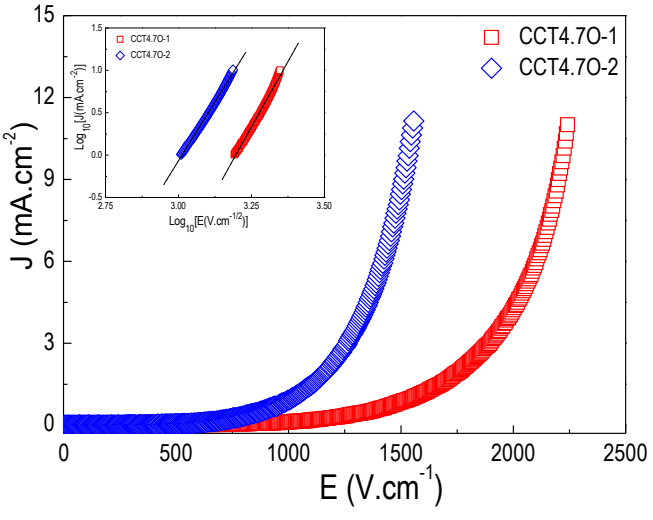

Figure 7. (a) *J- E* characteristics at room temperatures of CCT4.7O-1 and CCT4.7O-2 ceramics; inset shows plot of log (*J*) versus log (*E*) of both CCT4.7O ceramics, the solid lines are the best fit to Eq. $I=V^{a}$.

4. Conclusion

CCT4.7O powder of perovskite structure as revealed by the XRD results can be successfully prepared by calcination the CCT4.7O precursor powder obtained by the polymer pyrolysis method at 850 °C for 6 h in air. The second phases of TiO_2 and CuO are found in the precursor powder. The CCT4.7O-1 and CCT4.7O-2 ceramics are

prepared by sintering the obtained CCT4.7O powder at a temperature of 1060 ˚C for 6 and 10 h in air, respectively. The XRD results indicate the perovskite structure of both ceramics with the observed second phases of TiO_2 and CuO. Increasing sintering time can reduce the CuO second phase and increase the grain size of the CCT4.7O ceramic. From the dielectric measurements, it is found that higher sintering time can result in the higher dielectric constant with the low loss tangent. The CCT4.7O-2 ceramic particularly exhibits the giant dielectric constant (ε') value of approximately 31,908 with the low loss tangent ($\tan\delta$) value of 0.03 at 30 ˚C and 1 kHz and displays a temperature coefficient less than ±15% in the temperature range of −50 – 100 ˚C. The non-linear coefficients (α) of both ceramics are closely related to the sintering temperature, dielectric properties and grain boundary resistance (R_{gb}) that can be attributed to the variation in the height of the Schottky barriers.

5. Acknowledgement

This work was financially supported by Rajamangala University of Technology Rattanakosin Wang Klai Kangwon Campus, Thailand (Grant No. Inno 004/2557).

6. References

1 Chung SY, Kim ILD, Kang SJL. Strong Non-Linear Current–Voltage Behaviour in Perovskite-Derivative Calcium Copper Titanate. Nat. Mater. 2004; 3: 774.

2 Adams TB, Sinclair DC, West AR. Characterization of grain boundary impedances in fine- and coarse-grained $CaCu_3Ti_4O_{12}$. Phys. Rev. B. 2006; 73: 094124.

3 Sinclair DC, Adams TB, Morrison FD, West AR. $CaCu_3Ti_4O_{12}$: one-step internal barrier layer capacitor. Appl. Phys. Lett. 2002;80: 2153–2155.

4 Krohns S, Lunkenheimer P, Ebbinghaus SG, Loidl A. Colossal dielectric constants in single-crystalline and ceramics $CaCu_3Ti_4O_{12}$ investigated by broadband dielectric spectroscopy. J. Appl. Phys. 2008;103: 037602.

5 Ramirez MA, Bueno PR, Tararam R, Cavalheiro AA, Longo E, Varela JA. Evaluation of the effect of the stoichiometric ratio of Ca/Cu on the electrical and microstructural properties of the $CaCu_3Ti_4O_{12}$ polycrystalline system. J. Phys. D: Appl. Phys. 2009;2: 185503.

6 Si W, Cruz EM, Johnson PD, Barnes PW, Woodward P, Ramirez AP. Epitaxial thin films of the giant-dielectric-constant material $CaCu_3Ti_4O_{12}$ grown by pulsed-laser deposition Appl. Phys. Lett. 2002;81: 2056.

7 Amaral F, Rubinger CPL, Henry F, Costa LC, Valente MA, Timmons AB. Dielectric properties of polystyrene–CCTO composite. J. Non-Cryst. Sol. 2008;354: 5321.

8 Mu CH, Liu P, He Y, Zhou JP, Zhang HW. An effective method to decrease dielectric loss of $CaCu_3Ti_4O_{12}$ ceramics. J. Alloys Compd. 2009;471: 137.

9 Thongbai P, Putasaeng B, Yamwong T, Maensiri S. Modified giant dielectric properties of samarium doped $CaCu_3Ti_4O_{12}$ ceramics. Mater. Res. Bull. 2012; 47: 2257–2263.

10 Patterson EA, Kwon S, Huang CC. Effects of ZrO_2 additions on the dielectric properties of $CaCu_3Ti_4O_{12}$. Appl. Phys. Lett. 2005;87: 182911.

11 Thomas P, Dwarakanath K, Varma KBR. Effect of calcium stoichiometry on the dielectric response of $CaCu_3Ti_4O_{12}$ ceramics. J. Eur. Ceram. Soc. 2012;32: 1681–1690

12 ShriPrakash B, Varma KBR. The influence of the segregation of Cu-rich phase on the microstructural and impedance characteristics of $CaCu_3Ti_4O_{12}$ ceramics. J. Mater. Sci. 2007;42: 7467.

13 Fang TT, Mei LT. Evidence of Cu deficiency: a key point for the understanding of the mystery of the giant dielectric constant in $CaCu_3Ti_4O_{12}$. J. Am. Ceram. Soc. 2007;90: 638–40.

14 Chen K, Liu YF, Gao F, Du ZL, Liu JM, Ying XN, et al. Ti deficiency effect on the dielectric response of $CaCu_3Ti_4O_{12}$ ceramics. Solid State Commun. 2007;141:440–4.

15 Lin YH, Cai J, Li M, Nan CW. High dielectric and nonlinear electrical behaviors in TiO_2-rich $CaCu_3Ti_4O_{12}$ ceramics. Appl. Phys. Lett. 2006;88: 172902–4.

16 Liu J, Sui Y, Duan C, Mei WN, Smith RW, Hardy JR. $CaCu_3Ti_4O_{12}$: Low-temperature synthesis by pyrolysis of an organic solution. Chem. Mater. 2006;18: 3878.

17 Liu J, Smith RW, Mei WN. Synthesis of the giant dielectric material $CaCu_3Ti_4O_{12}$ by wet chemistry methods. Chem. Mater. 2007;19: 6020.

18 Thongbai P, Putasaeng B, Yamwong T, Maensiri S**.** Improved dielectric and non-ohmic properties of $Ca_2Cu_2Ti_4O_{12}$ ceramics prepared by a polymer pyrolysis method**.** J. Alloys Compd. 2011; 509: 7416–7420.

19 Swatsitang E, Niyompan A, Putjuso T. Giant dielectric, low dielectric loss, and non-ohmic properties of nanocrystalline $CaCu_3Ti_4O_{12}$. J. Mater. Sci.: Mater. Electron. 2013; 24: 3514.

20 Mohamed JJ, Hutagalung SD, Ain MF, Ahmad ZA. Effect of excess TiO_2 in $CaCu_3Ti_4O_{12}$ on the microstructure and dielectric properties. J. Ceram. Process. Res. 2011; 12: 496-499.

21 Li T, Fang K, Hao J, Xue Y, Chen Z. The effect of Ca-rich on the electric properties of $Ca_{1+x}Cu_{3-x}Ti_4O_{12}$ polycrystalline system. Mat. Sci. Eng. B. 2011;176: 171–176

22 Zhao J, Liu J, Ma G. Preparation, characterization and dielectric properties of $CaCu_3Ti_4O_{12}$ Ceramics. Ceram. Int. 2012; 38: 1221–1225.

23 Shao SF, Zhang JL, Zheng P, Zhong WL, Wang CL. Microstructure and electrical properties of $CaCu_3Ti_4O_{12}$ ceramics, J. Appl. Phys. 2006;99: 084106.

24 Li M, Feteira A, Sinclair DC. Relaxor ferroelectric-like high effective permittivity in leaky dielectrics/oxide semiconductors induced by electrode effects: A case study of CuO ceramics. J. Appl. Phys. 2009;105: 114109.

25 Zhang JL, Zheng P, Wang CL, Zhao ML, Li JC, Wang JF. Dielectric dispersion of $CaCu_3Ti_4O_{12}$ ceramics at high temperatures. Appl. Phys. Lett. 2005; 87: 142901.

26 Adams TB, Sinclair DC, West AR. Influence of Processing Conditions on the Electrical Properties of $CaCu_3Ti_4O_{12}$ Ceramics. J. Am. Ceram. Soc. 2006; 89: 3129.

27 Sun DL, Wu AY, Yin ST. Structure, Properties, and Impedance Spectroscopy of $CaCu_3Ti_4O_{12}$ Ceramic s Prepared by Sol–Gel Process. J. Am. Ceram. Soc. 2008;91: 169

28 Felix AA, Orlandi MO, Varela JA. Schottky-type grain boundaries in CCTO ceramics. Solid State Commun. 2011; 151: 1377.